RAPID COMMUNICATION

Velocity-selective spectroscopy measurements of Rydberg fine structure states in a hot vapor cell*

Jun He(何军)[1,2,3], Dongliang Pei(裴栋梁)[1,2], Jieying Wang(王杰英)[1,2], and Junmin Wang(王军民)[1,2,3,†]

[1] State Key Laboratory of Quantum Optics and Quantum Optics Devices, Shanxi University, Tai Yuan 030006, China
[2] Institute of Opto-Electronics, Shanxi University, Tai Yuan 030006, China
[3] Collaborative Innovation Center of Extreme Optics, Shanxi University, Tai Yuan 030006, China

(Received 23 June 2017; revised manuscript received 9 August 2017; published online 30 September 2017)

A velocity-selective spectroscopy technique for studying the spectra of Rydberg gases is presented. This method provides high-resolution spectrum measurements. We present experimental results for a ladder system $6S_{1/2} \rightarrow 6P_{3/2} \rightarrow nS(D)$ electromagnetically-induced transparency involving highly-excited Rydberg states. Based on a radio-frequency modulation technique, we measure the hyperfine structure splitting of intermediate states and the fine structure splitting of Rydberg states in a room temperature ^{133}Cs vapor cell. The experimental data and theoretical predictions show excellent agreement.

Keywords: Rydberg atom, fine structure, electromagnetically-induced transparency, velocity-selective spectroscopy

PACS: 32.80.Ee, 31.15.aj, 32.30.Bv **DOI:** 10.1088/1674-1056/26/11/113202

1. Introduction

The Rydberg atom possesses one electron in a very highly excited state, exemplifying a perfect quantum system with macroscopic size. Rydberg atoms have recently received considerable attention because of their great polarizability, strong dipole–dipole coupling, and long lifetime. The great polarizability indicates a sensitivity to electric fields, which makes Rydberg atoms very promising systems for producing high-precision field sensors, similar to the way in which the realization of nonlinear optical effects is used to obtain measurements of single photons nondestructively.[1–4] The strong dipole–dipole interaction renders Rydberg atoms promising candidates for implementation of protocols realizing quantum gates or efficient multi-particle entanglement for quantum information processing.[5–7] For quantum information applications, nondestructive detection of the Rydberg state is preferable. Electromagnetically induced transparency (EIT) is a nondestructive quantum interference effect with a narrow, subnatural linewidth,[8,9] which provides a detection technique with no absorption and allows dissipation-free sensing of the desired atomic resonance. Therefore, EIT can be used to control the transmission properties of an atomic ensemble with very weak switching fields. The subnatural linewidth EIT effect thus makes it possible to precisely measure the Rydberg series of energy levels. In recent experiments, EIT has been used to observe the Rydberg dipole blockade in ensembles of atoms, and it has been proposed to directly observe the dipole blockade using EIT as well as vector microwave electrometry.[10–12]

Great progress has also been made toward a ladder configuration of the Rydberg states in room temperature vapor cells. Experiments are being done to advance a precise optical spectrum technique to resolve the Rydberg states.[9,13–19] This is not only a very effective method for optical detection of the Rydberg states, but also a good way to measure optical non-linearity owing to the strong interaction between Rydberg atoms. The EIT signal intensity is limited primarily by the weak transition probability amplitude of the Rydberg states, while the signal noise arises from the phase and intensity noise of the laser.[20]

Using room temperature atom systems to make absolute energy shift measurements is difficult, especially for large-scale changes in the principal quantum number. In the present work, we present experimental results for a ladder system EIT involving highly-excited Rydberg states. Based on a radio-frequency (RF) modulation technique, we measured the velocity dependence of the hyperfine splitting of intermediate states and the fine structure splitting of Rydberg states in a room temperature ^{133}Cs vapor cell. Using velocity-selective spectroscopy combined with a RF modulation technique to measure the relative energy shift requires only an interval of the spectrum that is accurately distinguishable, where the measurement resolution can be made sensitive to a RF and a spectroscopy linewidth.[17]

An external cavity diode laser with a wavelength of $\lambda_p =$

*Project supported by the National Natural Science Foundation of China (Grant Nos. 61475091 and 61227902), the National Key Research and Development Program of China (Grant No. 2017YFA0304502), and the Scientific and Technological Innovation Programs of Higher Education Institutions in Shanxi, China (Grant No. 2017101).

†Corresponding author. E-mail: wwjjmm@sxu.edu.cn

© 2017 Chinese Physical Society and IOP Publishing Ltd

852 nm was used as the probing laser, with a typical linewidth in the megahertz scale. Infrared light from a diode laser with a wavelength of 1018 nm was amplified up to 5 W by a fiber amplifier, and the output beam was frequency doubled in a periodically-poled KTP crystal ($KTiOPO_4$) to produce a $\lambda_c = 509$ nm laser. The 852 and 509 nm-wavelength beams were then circularly polarized and overlapped in the cell with a counterpropagating configuration. The cell was tens of millimeters. The 852 nm-wavelength laser was locked to one of the $6S_{1/2} \rightarrow 6P_{3/2}$ hyperfine transitions via saturated absorption spectroscopy, and the laser wavelength was modulated by a waveguide phase-type electro-optic modulator. The 509 nm-wavelength enhanced doubling cavity was stabilized to the 1018 nm laser using the Pound–Drever–Hall RF modulation sideband method[21] and was fed back to a piezoelectric transducer (PZT). The entire system benefitted from ultra-stable mirror mounts to suppress noise. The model of the RF function generator (E8257D, Agilent Technologies) was locked to a rubidium clock (PRS10, Stanford Research Systems).

For a three-level ladder-type EIT, the matrix element ρ_{21} can be derived by solving the steady-state optical Bloch equations using a perturbation approximation in the weak probe field regime. Taking into account the Doppler effect and the Boltzmann velocity distribution, the EIT spectral line shape when applying an approximate expression for susceptibility can be written as

$$\chi(\upsilon)\mathrm{d}\upsilon = \frac{4\mathrm{i}\hbar g_{21}^2/\varepsilon_0}{\gamma_{21} - \mathrm{i}\Delta_\mathrm{p} - \mathrm{i}\dfrac{\omega_\mathrm{p}}{c}\upsilon + \dfrac{\Omega_\mathrm{c}^2/4}{\gamma_{31} - \mathrm{i}(\Delta_\mathrm{p} + \Delta_\mathrm{c}) - \mathrm{i}(\omega_\mathrm{p} \pm \omega_\mathrm{c})\upsilon/c}} N(\upsilon)d\upsilon,$$

where c is the speed of light; υ is the atomic velocity along the direction of the probe beam , "+" ("−") represents the co- (counter-) propagation configuration; Ω_p and Ω_c are the probe and coupling laser Rabi frequencies, respectively; $\Delta_\mathrm{p} = \omega_\mathrm{p} - \omega_{12}$ and $\Delta_\mathrm{c} = \omega_\mathrm{c} - \omega_{23}$ are the probe and coupling laser detunings, respectively; $N(\upsilon)\mathrm{d}\upsilon = (N_0 u^{-1}\pi^{-1/2})\mathrm{e}^{-x}\mathrm{d}\upsilon$ is the number density of atoms with velocity υ; $x = \upsilon^2/u^2$ and $u = \sqrt{kT/m}$, where k is the Boltzmann constant, T is the temperature, $\hbar$ is Planck's constant, and m is the mass of the ^{133}Cs atom; γ_{21} and γ_{31} are the natural widths of the intermediate and upper states, respectively; and g_{21} is the dipole moment matrix element.

Figure 1 shows the energy levels associated with the ladder-type Rydberg EIT. The EIT signal is observed by scanning the frequency of the $\lambda_c = 509$ nm coupling laser while locking the frequency of the $\lambda_p = 852$ nm probe laser. The background-free EIT spectrum with its high signal-to-noise ratio is a benefit for the low-noise laser system and the very weak laser power, which decreases the intensity noise and phase noise. Figure 2 shows the EIT signal of the hyperfine splitting of the intermediate state originating from the non-stationary atoms at room temperature. The center peak of the red line represents the $6S_{1/2}(F = 4) \rightarrow 6P_{3/2}(F' = 4) \rightarrow 43S$ resonance transition. Taking the velocity distribution into account, specific velocity group atoms are in resonance with the probing laser and coupling laser due to the Doppler effect, which results in the $6S_{1/2}(F = 4) \rightarrow 6P_{3/2}(F' = 3) \rightarrow 43S$ and $6S_{1/2}(F = 4) \rightarrow 6P_{3/2}(F' = 5) \rightarrow 43S$ transitions, respectively. In cases of RF bandwidth modulation, those that modulate the laser bandwidth frequencies also resonate with specific velocity groups of atoms. Such an effect is clearly sensitive to the modulation bandwidth frequency. All EIT signals of the intermediate states are observed because of the existence of different velocity classes of atoms. The EIT signals are observable upon averaging over a thermal velocity distribution. For a thermal ensemble, the residual Doppler averaging due to wavelength mismatch of the probe and coupling laser leads to the hyperfine splitting of the $5P_{3/2}$ states scale as $\Delta_c = (1 - \lambda_p/\lambda_c)\Delta_p$. For atoms with velocity υ moving in the same direction as the probe field, the detuning of the probe laser is $\Delta_p' \rightarrow -\omega_p \cdot \upsilon/c$ and that of the coupling laser is $\Delta_c' = \Delta_p' \cdot \omega_c/\omega_p$. Setting the transition frequency of $6S_{1/2}(F = 4) \rightarrow 6P_{3/2}(F' = 4) \rightarrow 42S$ as the reference frequency, the atoms with specific velocity groups $\upsilon_{4-4'}$ and $\upsilon_{4-3'}$ (where $\upsilon_{4-4'}/c = 251.0$ MHz and $\upsilon_{4-3'}/c = 452.2$ MHz) result in a resonance with other hyperfine states of $F = 4 \rightarrow F' = 4$ and $F = 4 \rightarrow F' = 3$, respectively. If the frequency of the 509 nm-wavelength coupling field matches these specific atoms groups to the levels of 43S, the Rydberg EIT signal can be detected, as shown in Fig. 2. The relative intensity of the transparency peaks under multi-intermediate levels of the ladder-type EIT depends on the population in the intermediate states.

The RF modulation combined with a velocity selection scheme can further tune the EIT peaks via Doppler shifts, which depend on the Boltzmann factor $\exp(\hbar\Delta/kT)$ and can be used to measure the peak splitting. The spectral resolution is limited by the EIT linewidth of the optical detection and so on. The signal intensity increases with the coupling and probe lasers' power, while the linewidth also increases. In the limit of a relatively high power for the coupling and the probe field, the observed EIT linewidth is ~ 9 MHz, including the $6P_{3/2}$ natural line width of 5.2 MHz, and the wavelength mismatch broadening of ~ 9 MHz for the case of a ladder system EIT with probing laser $\lambda_p = 852$ nm and coupling laser

$\lambda_c = 509$ nm. The dips in the enhanced absorption that are observed on both wings of the EIT signal originate from the residual Doppler effect, owing to a wavelength mismatch of the probe and the coupling lasers.

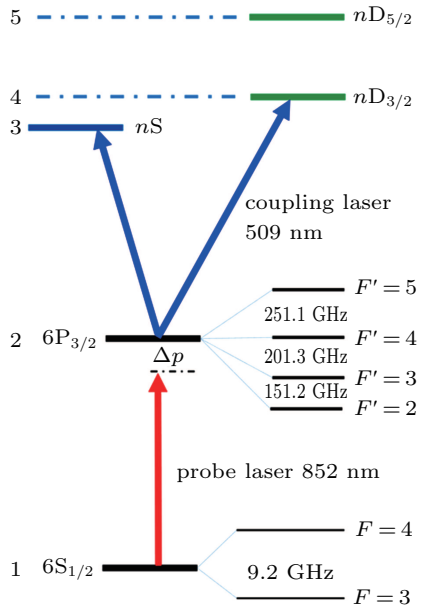


Fig. 1. (color online) Energy level schematic of the cascade-type electromagnetically induced transparency (EIT) of ^{133}Cs. The $\lambda_p = 852$ nm probe laser is frequency-stabilized to the hyperfine transition to measure the absorption on the $6S_{1/2}(F = 4) \rightarrow 6P_{3/2}(F' = 5)$ transition, while the $\lambda_c = 509$ nm laser beam is coupled to the 6P$\rightarrow n$S(D) transition.

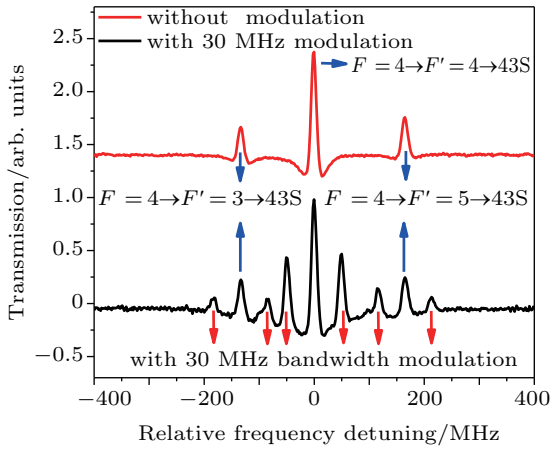


Fig. 2. (color online) EIT spectra across the principal quantum number $6S_{1/2}(F = 4) \rightarrow 6P_{3/2}(F') \rightarrow 43S$ transition with and without RF bandwidth modulation. The probe laser is resonant to the transition of $6S_{1/2}(F = 4) \rightarrow 6P_{3/2}(F' = 4)$. The coupling laser frequency is changed for scanning across the allowed transitions. The Rabi frequencies of the probe laser and coupling laser are ~ 1 MHz and ~ 10 MHz, respectively.

Figure 3 shows typical nD Rydberg state spectra, where the signal splitting decreases with the principal quantum number n. For a cesium atom at room temperature, the peak of $6S_{1/2}(F = 4) \rightarrow 6P_{3/2}(F' = 5) \rightarrow 59D_{5/2}$ overlaps with the peak of $6S_{1/2}(F = 4) \rightarrow 6P_{3/2}(F' = 3) \rightarrow 59D_{3/2}$, which arises from the fine-structure splitting of the Rydberg state and the hyperfine splitting of $6P_{3/2}(F')$. In the condition wherein $n = 59$, the peaks of $6S_{1/2}(F = 4) \rightarrow 6P_{3/2}(F' = 5) \rightarrow 59D_{5/2}$ and $6S_{1/2}(F = 4) \rightarrow 6P_{3/2}(F' = 3) \rightarrow 59D_{3/2}$ overlap. The strong interaction of the Rydberg states may cause their fine-structure peaks to shift. The RF modulation combined with a velocity selection scheme can be used to measure the peak splitting, where the resolution is only limited by the linewidth of the optical detection.

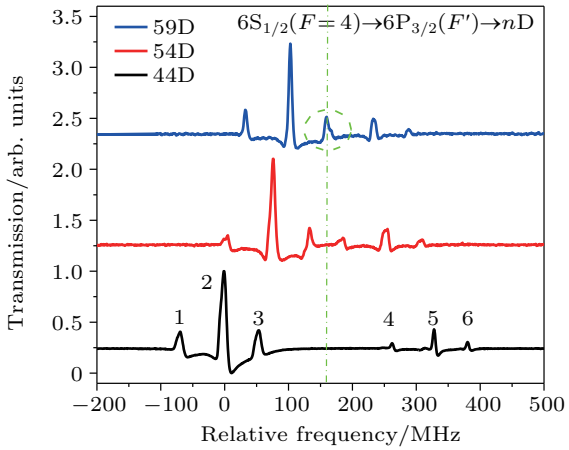


Fig. 3. (color online) Typical $6S_{1/2}(F = 4) \rightarrow 6P_{3/2}(F') \rightarrow n$D EIT spectra of the hyperfine splitting of intermediate states and fine structure splitting of Rydberg states. Because of the Rydberg splitting, the $D_{3/2}$ and $D_{5/2}$ states scale with $\Delta_c = (1 - \lambda_p/\lambda_c)\Delta_p$. The peaks labeled 1–3 respectively represent $F = 4 \rightarrow F' = (3,4,5) \rightarrow nD_{5/2}$, and the peaks labeled 4–6 respectively represent $F = 4 \rightarrow F' = (3,4,5) \rightarrow nD_{3/2}$. The horizontal coordinate is calibrated using the modulation sidebands of the $\lambda = 509$ nm laser. The green dashed line shows the peak overlap of the $6S_{1/2}(F = 4) \rightarrow 6P_{3/2}(F' = 5) \rightarrow 59D_{5/2}$ and $6S_{1/2}(F = 4) \rightarrow 6P_{3/2}(F' = 3) \rightarrow 59D_{3/2}$. The Rabi frequencies of probe laser and coupling laser are ~ 1 MHz and ~ 1 MHz, respectively.

Figure 4 shows the dependence of the fine structure and hyperfine structure on the principal quantum number n. The vertical coordinate is calibrated by the modulation sidebands. In the case of the hyperfine structure of the intermediate states, the spectral splitting depends upon a Doppler effect and the principal quantum number n, and the spectrum for small n is dominated by the $D_{3/2}$ and $D_{5/2}$ states. In the case of the fine structure of the Rydberg states, the spectral splitting depends sensitively on n and appears to overlap with the spectra of other states as the principal quantum number increases. Here, we use velocity-selective spectroscopy with RF modulation as a reference to calibrate the Rydberg fine-structure states in the room temperature vapor cell, where the RF frequency precision is smaller than 1 Hz for long time scales and the EIT linewidth is smaller than 9 MHz. The dominant deviations observed between the experimental and calculated results may arise from the nonlinear correspondence of the PZT while scanning the 509 nm-wavelength cavity.

Usually, it is difficult to observe the fine structure of the high principal quantum number Rydberg states because the spectral intensity is very weak in the limit of the Boltzmann velocity distribution. The EIT signal intensity depends on the

intensity and detuning of the laser, while the signal-to-noise ratio depends on the laser intensity noise and phase noise. The origin of the transmittance signal includes the EIT, two-photon absorption (TPA), double-resonance optical pumping (DROP) and single-resonance optical pumping (SROP), for special experimental parameters. In the case of an open atomic configuration, the magnitudes of the transmittance spectra slowly decrease compared with that of a cycling transition, owing to optical pumping. In the case of the closed ladder-type atomic system, EIT dominates TPA under the conditions of a weak probe and strong coupling laser power. The SROP and DROP are considered to be single- or two-photon resonance pumping and spontaneously decay into other hyperfine states that depend on the detuning of the probing and coupling lasers, and are therefore weak under the condition of weak intensity and far detuning.

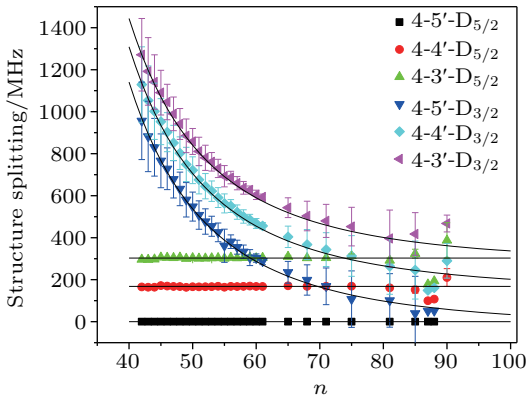


Fig. 4. (color online) Spectral splitting as a function of the principal quantum number n from experimental values (color symbol) and theoretical results (black line). The deviations are the bias errors between the theoretical and measured data. It appears as if the 4-5′-nD$_{5/2}$ transition frequencies are independent of quantum number n, this is because the 4-5′-nD$_{5/2}$ is chosen as the reference frequency.

For our parameters, the power of the probe laser is on the order of hundreds of nanowatts, and the phase noise has been significantly suppressed. As the Doppler shift compensates the frequency detuning of the probe laser, atoms in a typical velocity group begin to resonate with the probe laser, whereupon the six EIT peaks with considerable signal-to-noise are observed. Owing to the Doppler effect, the probe laser resonant with $F = 4 \rightarrow F' = 5$ is a cycling transition that can suppress the SROP and DROP. For the larger absolute frequency detuning, we have achieved an optimized transmission signal and the linewidth exhibits a small increase, which signifies that the EIT signal is dominant.

We observed hyperfine-structure splitting of the intermediate states and fine-structure splitting of the Rydberg states. The measured results deviate from the theoretical results at higher principal quantum n values, which may arise from strong interaction between the highly-excited Rydberg atoms, which induces energy state shifts.[5–7] The interactions between the S and D states are repulsive or attractive depending on the special Rydberg states.[22] Studies of Rydberg atom interactions require extremely precise optical detection. Energy shifts arising from the van der Waals and dipole–dipole interactions, Forster resonance, etc., scale in tens of megahertz, and with the ~ 9 MHz-resolution bandwidth, it is difficult to achieve accurate measurements at such frequency scales. Our experiments are limited by the noise arising from the laser intensity noise and phase noise. Although the homodyne technique is effective in decreasing probe laser phase noise,[23] the crucial points are narrowing the linewidth of the optical detection by suppressing both the intensity and phase noise.

In summary, we demonstrated measurement of the fine structure of the Rydberg states by velocity-selective spectroscopy combined with RF bandwidth modulation. We presented experimental results for a ladder system $6S_{1/2} \rightarrow 6P_{3/2} \rightarrow n$S(D) EIT involving highly excited Rydberg states in a room temperature ^{133}Cs vapor cell. The experimental results show that this optical technique can be used to measure the Rydberg series of an energy level. The optical spectrum resolution ~ 9 MHz is limited by the linewidth of the EIT signal and the noise of the lasers, which can be mitigated by decreasing the laser phase noise, given weak laser power. Velocity-selective spectroscopy combined with RF bandwidth modulation is an effective technique for studying interval spectrum splitting. It is not only an effective method for optical detection of the fine structure of Rydberg states, but it is also a good way to measure the strong interactions between Rydberg atoms at weak levels of laser power. Moreover, the non-destructive EIT detection demonstrated herein makes it possible to advance this technique to achieve high-precision measurements of electric fields and microwaves at the single-photon level.

References

[1] Pritchard J D, Maxwell D, Gauguet A, Weatherill K J, Jones M P A and Adams C S 2010 *Phys. Rev. Lett.* **105** 193603
[2] Dudin Y O and Kuzmich A 2012 *Science* **336** 887
[3] Peyronel T, Firstenberg O, Liang Q Y, Hofferberth S, Gorshkov A V, Pohl T, Lukin M D and Vuletić V 2012 *Nature* **488** 57
[4] Maxwell D, Szwer D J, Paredes-Barato D, Busche H, Pritchard J D, Gauguet A, Weatherill K J, Jones M P A and Adams C S 2013 *Phys. Rev. Lett.* **110** 103001
[5] Saffman M, Walker T G and Moelmer K 2010 *Rev. Mod. Phys.* **82** 2313
[6] Jaksch D, Cirac J I, Zoller P, Rolston S L, Cote R and Lukin M D 2000 *Phys. Rev. Lett.* **85** 2208
[7] Lukin M D, Fleischhauer M, Cote R, Duan L M, Jaksch D, Cirac J I and Zoller P 2001 *Phys. Rev. Lett.* **87** 037901
[8] Fleischhauer M, Imamoglu A and Marangos J P 2005 *Rev. Mod. Phys.* **77** 633
[9] Mohapatra A K, Jackson T R and Adams C S 2007 *Phys. Rev. Lett.* **98** 113003
[10] Müller M, Lesanovsky I, Weimer H, Buchler H P and Zoller P 2009 *Phys. Rev. Lett.* **102** 170502

[11] Bason M G, Tanasittikosol M, Sargsyan A, Mohapatra A K, Sarkisyan D, Potvliege R M and Adams C S 2010 *New J. Phys.* **12** 065015
[12] Barredo D, Kubler H, Daschner R, Löw R and Pfau T 2013 *Phys. Rev. Lett.* **110** 123002
[13] Mack M, Karlewski F, Hattermann H, Höckh S, Jessen F, Cano D and Fortágh J 2011 *Phys. Rev. A* **83** 052515
[14] Kübler H, Shaffer J P, Baluktsian T, Löw R and Pfau T 2010 *Nat. Photon.* **112** 16
[15] Miller A, Anderson D A and Raithel G 2016 *New J. Phys.* **1** 053017
[16] Jiao Y C, Han X X, Yang Z W, Li J K, Raithel G, Zhao J M and Jia S T 2016 *Phys. Rev. A* **94** 023832
[17] Xu W and DeMarco B 2016 *Phys. Rev. A* **93** 011801(R)
[18] Bao S X, Zhang H, Zhou J, Zhang L J, Zhao J M, Xiao L T and Jia S T 2016 *Phys. Rev. A* **94** 043822
[19] Tauschinsky A, Newell R, van Linden van den Heuvell H B and Preeuw R J C 2013 *Phys. Rev. A* **87** 042522
[20] Hsu M T L, Hétet G, Glöckl O, Longdell J J, Buchler B C, Bachor H A and Lam P K 2006 *Phys. Rev. Lett.* **97** 183601
[21] Black E D 2001 *Am. J. Phys.* **69** 79
[22] Schwettmann A, Crawford J, Overstreet K R and Shafferet J P 2006 *Phys. Rev. A* **74** 020701
[23] Kumar S, Fan H Q, Kübler H, Jahangiri A J and Shafferr J P 2017 *Opt. Express* **25** 8625